Electrical Power and Energy Systems 172 (2025) 111153

Contents lists available at ScienceDirect

International Journal of Electrical Power and Energy Systems

journal homepage: www.elsevier.com/locate/ijepes

Multi-dimensional evaluation and synergistic optimization for double-circuit distribution lines under transient events☆

Chakhung Yeung [a], Yuxuan Ding [a,*], Quan Zhou [a,*], Yaping Du [a], Huaifei Chen [b], Lei Jia [b], Song Zhang [c], Yue Li [c]

[a] Department of Building Environment and Energy Engineering, The Hong Kong Polytechnic University, Hong Kong, China
[b] State Key Laboratory HVDC Transmissions Technology, China Southern Power Grid, Guangzhou, 510700, China
[c] Guizhou Electric Power Research Institute, China Southern Power Grid, Guiyang, 546000, China

ARTICLE INFO

Keywords:
Distribution system
Lightning protection
Lightning-induced overvoltage
Multi-dimensional evaluation

ABSTRACT

Lightning-induced Overvoltage (LIOV) represents a critical factor impacting the stability and reliability of equipment in distribution systems. Despite its significance, existing studies lack systematic analysis of LIOV characteristics and protection strategies in 10 kV double-circuit distribution lines when adjacent circuits are struck by direct lightning stroke. This study aims to quantify the effects of Surge Arrester (SA) deployment density, Shielding Wire (SW) grounding intervals, and grounding resistance on LIOV, and to propose optimal protection schemes balancing performance and cost. A hybrid simulation model, based on the Partial Element Equivalent Circuit (PEEC) method with the Variable Time Step (VTS) strategy, was developed to simulate LIOV responses in a double-circuit distribution system. Lightning current waveforms were modeled by the Heidler function, and SAs were represented by IEEE-recommended frequency-dependent circuits. Results show that SA deployment with one-pole intervals enhances the one-phase flashover lightning withstand level from 1.7 kA to 3.9 kA. This performance is better than that of SW alone where three-pole grounded SW achieve a one-phase flashover lightning withstand level of 38.7 kA. Combining one-pole SA intervals with one-pole grounded SW reduces flashover rates by 30% while maintaining economic feasibility. The findings provide valuable theoretical support for practical lightning protection designs in double-circuit distribution systems.

1. Introduction

Lightning surges are among the primary causes of power system failures, particularly in distribution systems [1–3]. What distinguishes 10 kV distribution lines from high-voltage transmission lines is their inadequate insulation combined with their critical role in connecting modern power systems to end users. Among lightning-related faults, Lightning-induced Overvoltage (LIOV) is a primary cause of Flashovers (FOs) and outages in low-voltage networks [4–6]. With the rapid integration of distributed energy resources, the vulnerability of such systems to LIOV has increased, further underscoring the need for effective protection strategies [1,7–9]. Therefore, the issue of how to effectively prevent lightning strokes has quickly become a focus of attention in academic circles [10–12].

Experiments [2,13–15] and numerical simulations [16–19] have become the primary methods for evaluating the design of protection systems against LIOV in distribution networks. Due to the inherent risks and high costs associated with experiments involving natural lightning strokes, obtaining experimental data under varied conditions remains a challenge. Thus, in practical applications, numerical simulations are widely regarded as the most effective means of assessment.

Table 1 summarizes the main studies on LIOV in overhead lines. Diendorfer et al. [20] used the Agrawal time-domain method to calculate LIOV from nearby lightning while Nucci et al. [21,22] developed models based on channel base current initial conditions. Ishii et al. [23] highlighted the influence of soil conductivity and stroke location on terminal overvoltage magnitudes. Rachidi et al. [24] found leader electric

☆ The work leading to this paper was supported by China Southern Power Grid, China under project "Development of a Simulation Platform for the Transient Process of Strong Electromagnetic Pulse Coupling in New Energy Distribution Systems (Phase One) - Subproject 1: Research on Spatio-Temporal Multi-ScaleSimulation Technology for New Energy Distribution Networks Considering Probabilistic Risks of Strong Electromagnetic Pulses" (NO.GZKJXM20222352).

* Corresponding authors.
E-mail addresses: chakhung.yeung@connect.polyu.hk (C. Yeung), yx.ding@connect.polyu.hk (Y. Ding), q3zhou@polyu.edu.hk (Q. Zhou), yaping-du@polyu.edu.hk (Y. Du), chenhf@csg.cn (H. Chen), jialei@csg.cn (L. Jia), zhangsong@gzzy.csg.cn (S. Zhang), 1641356033@qq.com (Y. Li).

https://doi.org/10.1016/j.ijepes.2025.111153
Received 8 May 2025; Received in revised form 4 August 2025; Accepted 14 September 2025
Available online 1 October 2025

Table 1
Summary of existing studies on LIOV in overhead lines.

Authors	Research object	Method	Key findings	Limitations
Diendorfer et al. [20]	LIOV from nearby lightning strokes on overhead lines	Agrawal method in time-domain	Calculated LIOV by solving transmission line equations	1. Did not consider double-circuit systems 2. Ignored shielding devices
Nucci et al. [21,22]	LIOV from subsequent return strokes on distribution lines	Model based on channel base current	Subsequent strokes increase LIOV duration and peak value	1. Neglected soil resistivity variation 2. Did not account for grounding resistance effects
Ishii et al. [23]	LIOV influenced by soil conductivity and stroke location	Telegraph equation with electric field calculations	Soil conductivity significantly affects LIOV amplitude	1. Focused on single-circuit lines 2. No analysis of protection strategies
Rachidi et al. [24]	LIOV induced by dart leaders on overhead lines	Model considering leader electric field	Dart leaders produce higher-frequency LIOV components	1. Did not address double-circuit systems 2. Ignored direct stroke scenarios
Paulino et al. [25]	Sensitivity of LIOV to soil resistivity and line length	Agrawal model in MATLAB	LIOV increases with soil resistivity and line length	1. Ignored combined effects of SAs, SW, and grounding resistance 2. Did not consider double-circuit coupling
Cao et al. [26,29]	Cost-effectiveness of lightning protection for 10 kV lines	Techno-economic comparison model	Optimized SA/SW configurations based on economic analysis	1. Limited to single-circuit lines 2. No assessment of inter-circuit LIOV coupling
Christodoulou et al. [27]	150 kV Hellenic overhead transmission lines	Regional differentiation with multi-parameter optimization	Optimized parameters reduce lightning failure rates	1. Focuses on high-voltage lines
Ekonomou et al. [28]	150/400 kV Hellenic overhead transmission lines	Cost-related regional differentiation with parameter optimization	Balances cost and lightning performance in 150/400 kV lines	1. Limited to high-voltage lines

fields affect LIOV waveform characteristics. Paulino et al. [25] demonstrated the sensitivity of LIOV to soil resistivity and line length and Cao et al. [26] assessed the economic performance of protection schemes. Christodoulou et al. [27] proposed an optimization method for integrated grounding wire and Surge Arrester (SA) for Greek 150 kV lines to significantly reduce the lightning failure rate. Ekonomou et al. [28] considered cost factors and parameters, such as Shielding Wire (SW) height and verified the synergistic optimization effect of cost and lightning protection performance.

Despite these efforts, most studies focus on single-circuit lines or direct stroke impacts with limited analysis of LIOV coupling between double-circuit distribution lines so far, especially when one circuit is directly struck and overvoltage is induced in the adjacent circuit. Existing studies overlook the integrated effects of grounding resistance, SA deployment density and SW grounding intervals on LIOV in such configurations. Additionally, differentiated protection strategies tailored to double-circuit systems remain underdeveloped, leaving a critical gap in practical lightning protection design guidance.

Based on this, the hybrid Variable Time Step and Partial Element Equivalent Circuit (VTS-PEEC) method is used to calculate the LIOV on a 10 kV double-circuit distribution line in this paper. Specifically, the variation of the LIOV on Line II when Line I is struck by lightning stroke is analyzed. This paper examines the effects of different configurations of SAs, various grounding methods of the SW, and grounding resistance on the LIOV. The findings of this study provide theoretical support for improving lightning protection in distribution systems. The main contributions of this paper are as follows:

(1) Investigated systematically are LIOV characteristics in 10 kV double-circuit distribution lines, with a focus on overvoltage induced in the adjacent circuit when one circuit is directly struck by lightning stroke, addressing the research gap in existing literature regarding such scenarios.

(2) Quantified are the combined effects of SA deployment density, SW grounding intervals, and grounding resistance on LIOV mitigation.

(3) Proposed are optimal, regionally differentiated lightning protection strategies that balance technical performance and economic efficiency, with SA deployment intervals tailored to annual lightning density, soil resistivity, and network topology.

The remainder of the paper is organized as follows, with the main research route of this paper outlined in Fig. 1. Section 2 describes the model configuration, including line parameters, component models, and the hybrid VTS-PEEC simulation method. Section 3 analyzes LIOV characteristics on the adjacent circuit without additional protection. Section 4 investigates the influence of key parameters. Section 5 evaluates five protection strategies from both performance and cost perspectives. Finally, Section 6 summarizes the findings and outlines future work.

2. Model configuration and numerical methodology

2.1. Model configuration for surge simulation

To investigate the characteristics of the LIOV on distribution lines when a lightning stroke occurs on the adjacent circuit in a double-circuit configuration, this paper focuses on 10 kV unequally spaced parallel overhead lines in a distribution system, as illustrated in Fig. 2. The system consists of 22 poles, each separated by approximately 70 m. For Line I, the first 17 poles form a double-circuit structure, while Pole 18 to Pole 22 transition into a single-circuit configuration. The segment from Pole 1 to Pole 17 spans 1,122 m, whereas the section from Pole 18 to Pole 22 extends 391 m. Given that the study area is characterized by hilly terrain, Line I adopts an L-shaped layout from Pole 1 to Pole 22, whereas Line II follows a straight path from Pole 1 to Pole 17. The spacing between the two circuits is 2.5 m. At both ends of Line I, 10 kV distribution transformers are installed, whereas in Line II, these transformers are replaced with an equivalent capacitance.

The specific pole arrangement is illustrated in Fig. 3. The three-phase conductors are vertically aligned, with a spacing of 0.9 m between them. Phase C is positioned the lowest, 10 m above the ground. SW is installed directly above Phase A of Line I, maintaining a 1 m separation, and is grounded at each pole. The grounding electrodes are buried approximately 3 m underground. Each phase conductor follows the J/G1A-240/30 model, while the SW is modeled as GJ-35. The soil resistivity is approximately 190 $\Omega \cdot$ m, and the grounding resistance at each pole varies between 3 and 22 Ω. In this paper, 10 kV/200 kVA transformers are installed at both ends of Line I, while SAs are positioned only at the beginning and end of Line II. No matching impedance is applied at either end of the double-circuit line which is consistent with the actual configuration of 10 kV distribution lines in engineering practice. The results from Zhao et al. [30] have shown that the absence of matching impedance primarily affects waveform oscillations and wave tails rather than voltage peak values.

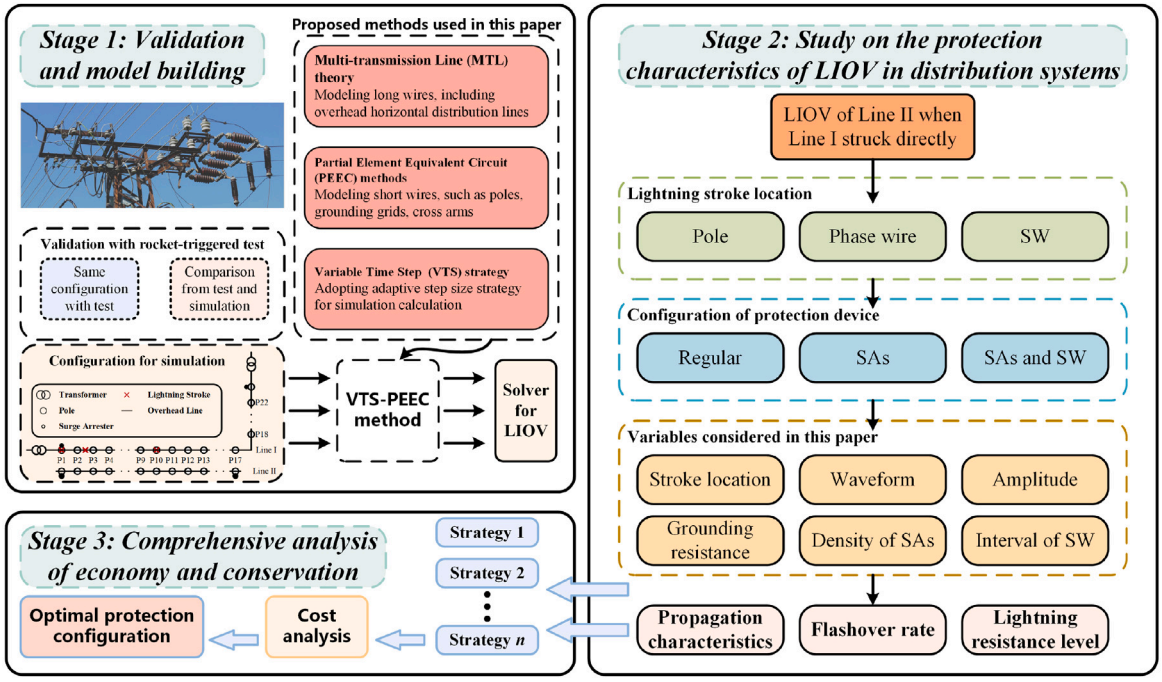

Fig. 1. Schematic diagram of the technical route studied in this paper.

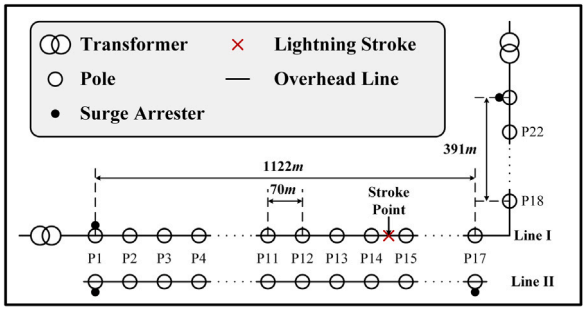

Fig. 2. Schematic of the test placement for a double-circuit distribution system.

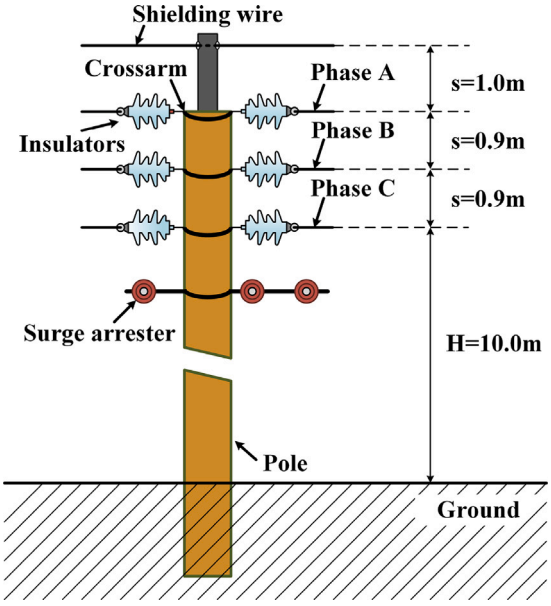

Fig. 3. Specific configuration of the pole used in this paper.

2.2. Surge simulation with a hybrid method

A hybrid VTS-PEEC method is adopted in this paper for transient analysis of distribution systems [31]. The system consists of three types of components, including short conductors, long conductors, and lumped parameter models. Detailed modeling of elements, such as crossarm and grounding wire, is handled by the short conductor model, which is well-suited for representation using the PEEC method [32]. The three-phase conductors and SW are treated as long conductors running parallel to the grounded surface. These components are not suitable for the PEEC method, so they are instead described using the Multi-Conductor Transmission Line (MTL) theory [33]. Note that, both models effectively account for grounding loss effects [34]. The strategy of using the VTS method greatly reduces the computation time of transient simulation, enhancing efficiency while preserving the modeling accuracy of conventional methods.

Electrical components in the distribution system, such as transformers, SAs, and insulators, are modeled using lumped parameter models commonly employed in simulation [32]. Since the surge energy at the medium-voltage is of concern, the distribution transformer is replaced by an equivalent capacitance of 0.5 nF [35]. The SA is modeled using frequency-dependent circuits recommended by IEEE [36], as shown in Fig. 4. The soil resistivity used in the case study is 190 Ω · m, which is consistent with the local environmental conditions, assuming that the soil is homogeneous.

The Critical Flashover Voltage (CFO) model, recommended by IEEE [37], assesses the FO status on an insulator, referring to the voltage level at which the insulator has a 50% probability of FO. The threshold level is typically assumed to be 1.5 times the CFO of lines, which is defined as follows:

$$CFO_{\text{ins}} = 1.5 \times CFO_{\text{line}} = 296 \text{ kV} \tag{1}$$

where CFO_{ins} and CFO_{line} are the CFO of insulator and line, respectively.

By applying basic circuit analysis methods, the VTS-PEEC model is combined with the circuit models of electrical components in the distribution system to formulate the node analysis equations of the distribution system, followed by time-domain numerical simulations to

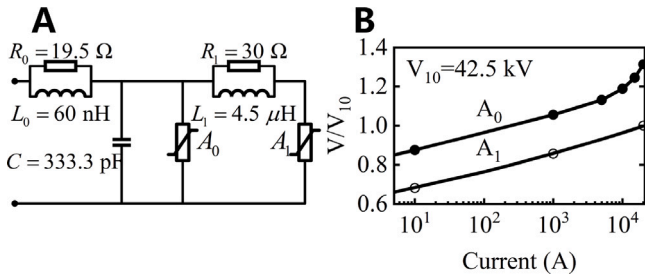

Fig. 4. Model of the SA used in this paper, with (a) equivalent circuit, and (b) V-I characteristic of the nonlinear resistors.

Table 2
Parameters of lightning current captured in the rocket-triggered lightning experiment.

Return stroke	Amplitude (kA)	Front time (μs)	Half-peak time (μs)
RS1	36.12	0.57	25.98
RS2	12.38	0.65	8.74
RS3	10.56	0.55	2.68
RS4	13.23	0.52	2.52
RS5	12.93	0.56	2.71
RS6	19.98	0.48	7.42
RS7	14.89	0.49	2.29
RS8	27.04	0.51	9.37
RS9	13.16	0.50	0.96

analyze the LIOV of the poles during a lightning stroke. For double-circuit lines, LIOV induced by direct lightning strokes arises primarily from electromagnetic coupling between parallel conductors, an effect amplified by the close spacing between lines and their interconnected structure. The PEEC method, which transforms electromagnetic field problems into circuit problems, enables transient simulation analysis by leveraging well-established circuit theory and techniques.

When a direct lightning stroke occurs on an adjacent line, the induced overvoltage on the nearby line stems from two key mechanisms captured in the PEEC equivalent circuit, including mutual potential coefficients, and mutual inductances. Mutual potential coefficients account for electric field coupling, where the electric field from the lightning current in the struck line induces charges on the adjacent line, creating scalar potential differences. Mutual inductances dominate magnetic field coupling, as the time-varying magnetic field generated by the lightning current induces vector potentials in the adjacent line via electromagnetic induction. These two coupling effects, electric and magnetic field interactions, act in concert to generate the induced overvoltage, with the PEEC method effectively capturing and quantifying them through its circuit-based modeling approach.

2.3. Model validation

The dataset utilized for validating the hybrid method in this study originates from a rocket-triggered lightning experiment conducted in June 2019 in Conghua, Guangdong Province, China. Nine direct Return Strokes (RS) from rocket-triggered lightning, designated F1906301713, were recorded on Phase C of Line I, specifically between Pole 14 and Pole 15, as shown in Fig. 2. The lightning current waveforms of RS1 to RS8 and their parameters are presented in Fig. 5 and summarized in Table 2. To evaluate the performance of the proposed hybrid computational method, a LIOV event was simulated on Phase C at Pole 10. The simulation results were compared against empirical observations from the rocket-triggered lightning experiments, as shown in Fig. 6.

The simulation results exhibit a strong consistency with the experimental observations, indicating that the hybrid method used in this paper is capable of accurately capturing the LIOV in the double-circuit distribution system. Note that the initial reverse polarity pulse observed prior to the first overvoltage peak is linked to the stepped leader phenomenon, which has not yet been represented in the lightning channel model used in this work. Further investigation into this aspect will be conducted to enhance the incorporation of the full electromagnetic effects.

Table 3
Calculation parameters without additional configuration.

Current waveform	Current amplitude (kA)	Grounding resistance (Ω)	Stroke point
First-return stroke	10	5	S1: Pole w SA
Subsequent return stroke	30	15	S2: Terminal line
	50	25	S3: Pole w/o SA
	80	35	S4: Central line
	100	50	

Table 4
Statistical analysis of positive and negative peak voltage along Line II (A first-return stroke occurs at S1).

Pole	Negative peak value (kV)			Positive peak value (kV)		
number	Phase A	Phase B	Phase C	Phase A	Phase B	Phase C
P2	−32.34	−33.34	−32.27	15.98	15.15	15.42
P3	−32.93	−34.81	−32.56	18.53	17.98	18.35
P4	−31.84	−33.69	−32.41	19.09	18.67	19.29
P5	−31.69	−33.31	−32.79	17.48	16.96	17.88
P6	−31.72	−33.16	−33.09	14.61	13.69	15.14
P7	−31.85	−33.09	−33.47	15.97	16.32	15.00
P8	−32.07	−33.11	−33.97	18.62	18.73	17.42
P9	−32.58	−33.39	−34.75	18.56	18.63	17.04
P10	−34.21	−34.25	−36.18	17.21	17.26	18.21
P11	−35.52	−35.75	−38.25	17.03	15.93	21.11
P12	−37.74	−37.55	−40.76	19.58	17.60	23.91
P13	−40.81	−40.14	−44.09	22.06	19.92	26.60
P14	−43.58	−42.44	−46.79	24.45	22.17	29.16
P15	−42.18	−40.78	−44.70	26.66	24.26	31.35
P16	−28.07	−27.20	−28.78	25.11	22.91	28.47

3. LIOV result without additional configuration

The propagation characteristics of LIOV on Line II of a 10 kV double-circuit distribution system, when a lightning stroke occurs on Line I, are investigated in this section. The specific calculation conditions are provided in Table 3. The typical waveforms of the first-return stroke and subsequent stroke, as illustrated in Fig. 7, are considered in this paper and modeled by the Heidler function [38].

A 10 kA first-return stroke directly impacting Pole 1, which is equipped with SAs, results in the LIOV variation of the three-phase along the poles of Line II, as shown in Fig. 8. The lightest color in Fig. 8 represents Pole 2 on the far left, while the darkest color corresponds to Pole 16 on the far right. The LIOV waveform of the three-phase on Line II is generally similar, both exhibiting a bipolar oscillation characteristic, which arises from electromagnetic coupling between the two circuits. There is an approximate 0.3 μs delay between the LIOV of different poles, indicating a certain time lag in the propagation of the voltage wave between the poles along the line. The statistical data of the positive and negative peak values are shown in Table 4. The dominance of negative peaks with positive peaks at 60% of negative amplitudes is attributed to the fast-rising front of the return stroke current. As shown in Table 2, the front time is 0.5 μs. It is also related to the nonlinear clamping effect of SAs at Pole 1. This aligns with the same finding from Ishii et al. [23], in which soil conductivity affects overvoltage polarity, though our double-circuit setup introduces stronger inter-phase coupling than single-circuit systems they studied. The consistent amplitude below 50 kV, as shown in Table 4, indicates baseline protection effectiveness but highlights vulnerability to higher current strokes such as 80 kA as later shown.

The peak value of the grounding current for Line II is shown in Fig. 9, where it can be observed that the peak value remains below

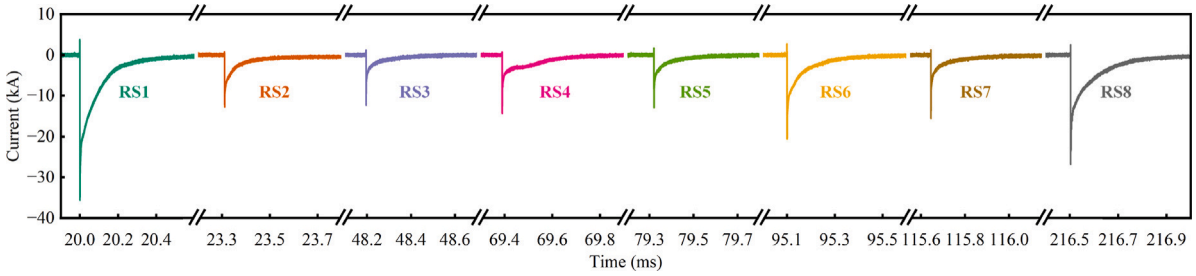

Fig. 5. Lightning current waveform, from event F1906301713, captured during the rocket-triggered lightning experiment.

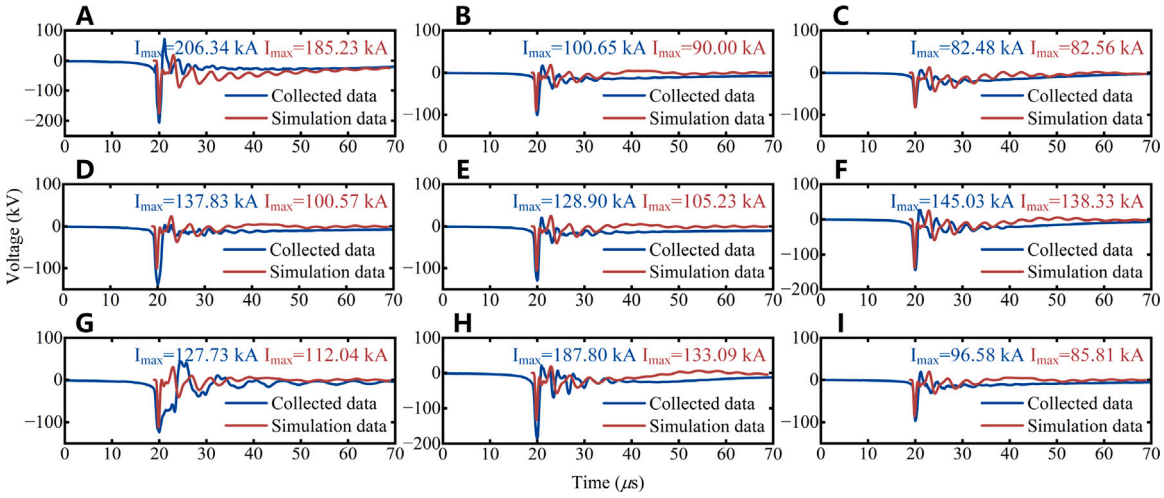

Fig. 6. Comparison of tested and simulated results for Phase C at Pole 10 on Line I, where (a) to (I) are RS1 to RS9, respectively.

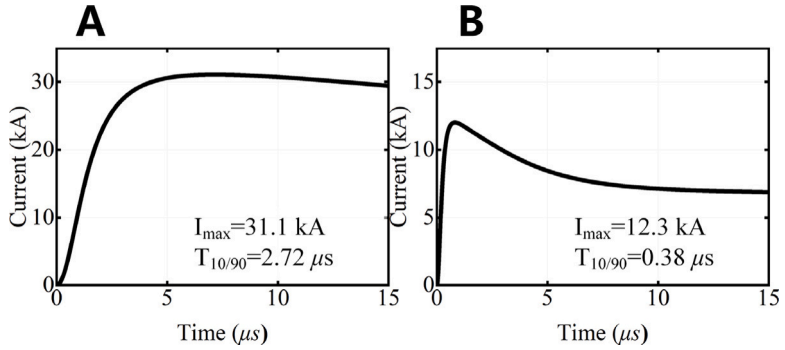

Fig. 7. Typical waveform and the parameters of (a) the first-return stroke and (b) the subsequent return stroke.

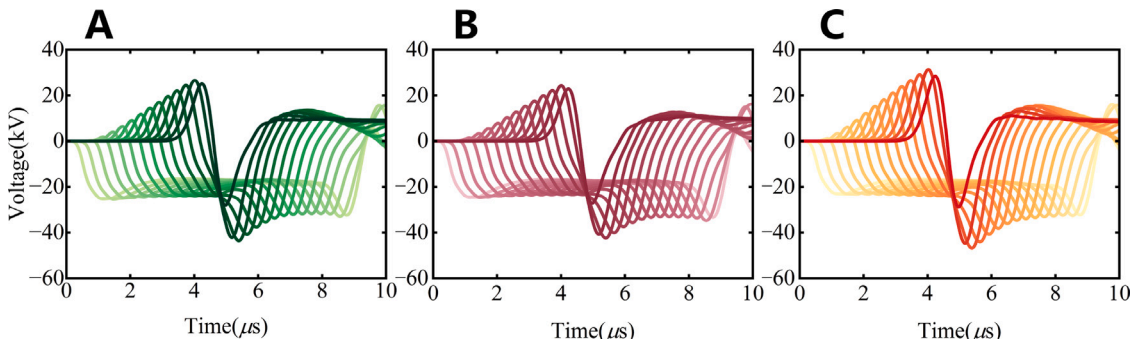

Fig. 8. Propagation characteristics of the three-phase voltage along Line II, where A to C represent Phases A, B, and C, respectively. (For interpretation of the references to color in this figure legend, the reader is referred to the web version of this article.)

Table 5
Description of lightning stroke points with different configurations of SAs.

Configuration	Lightning occurs on poles		Lightning occurs on lines	
of SAs	S1	S3	S2	S4
Regular	Pole 1	Pole 10		
Span three poles (3P)	Pole 14	Pole 16	Phase A between	Phase A between
Span two poles (2P)	Pole 16	Pole 14	Pole 2 and Pole 3	Pole 11 and Pole 12
Span one pole (1P)	Pole 16	Pole 13		

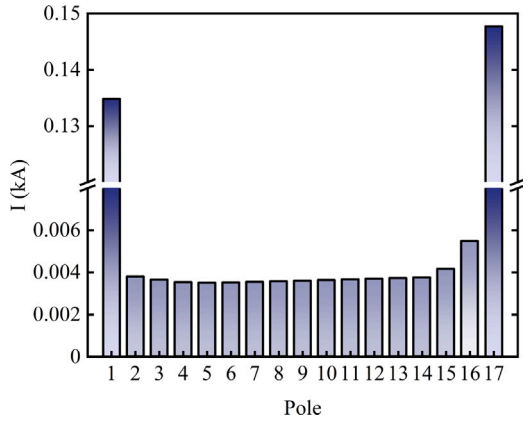

Fig. 9. Grounding current peak values at each pole of Line II.

1 kA at all times, without causing excessive impact on the line. The current is primarily handled by the SAs at both ends of Line II, successfully limiting its propagation to other poles and effectively preventing excessive current from entering the soil. SAs effectively divert current within a certain range, preventing severe overcurrent faults and playing a crucial protective role. When a lightning stroke impacts a pole, it is more likely to cause FO, especially on poles without SAs. However, since equipping every pole with SAs is often economically unfeasible, optimizing their configuration in the distribution system to enhance their ability to handle high currents is becoming increasingly important.

4. Influence of design parameters on LIOV

The LIOV on Line II is investigated in this section when different lightning protection strategies are implemented on Line I of a 10 kV double-circuit distribution system, considering the influence of various parameters on LIOV. The calculation conditions for LIOV are summarized in Table 3. Specifically, the lightning stroke points corresponding to different configurations of SAs are presented in Table 5, and the calculation conditions with an SW on Line I are shown in Table 6. The effects of factors, such as the interval of SAs, the grounding interval of the SW, and the grounding resistance on LIOV along Line II are analyzed.

4.1. Interval of SAs along the Line I

A 50 kA subsequent return stroke occurring at Pole 16 of Line I, results in the propagation characteristics of LIOV of Phase A along Line II under three different configurations, as shown in Fig. 10. In Fig. 10(a), with SAs installed across every three-pole span along Line I, a noticeable difference in waveform and amplitude is observed at Pole 15 and Pole 16, the closest to the stroke point, primarily due to the SA located at the Pole 17 of Line I. In the cases where SAs are installed every two-pole and one-pole spans of Line I, when lightning strokes occur on SA-equipped poles, the LIOV is shown in Fig. 10(b) and (c), respectively. The waveform features are similar for both configurations. The LIOV of Pole 16, closest to the lightning stroke point, exhibits a negative polarity. The LIOV of Pole 14 and Pole 15 initially drops to a negative peak, undergoes polarity reversal and rises to a positive peak, and finally oscillates back to zero. The LIOV at the remaining poles along Line II, from Pole 2 to Pole 13, exhibits the opposite behavior.

Table 6
Calculation parameters with SW.

Configuration of SAs	Ground span of SW	Lightning stoke point
Span three poles (3P)	Span three poles (3P)	Central SW between
Span one pole (1P)	Span one pole (1P)	P9 and P10 in Line I
	Every pole	

The comparison between the amplitude of LIOV along Line II, with SAs installed every two-pole and one-pole span on Line I, under a 50 kA subsequent return stroke occurring at Pole 16 of Line I is shown in Fig. 11. The amplitudes along Line II are similar, with lower amplitudes when SAs are installed across every one-pole span, providing more effective protection for the line against lightning. Whereas, the key issue is how to achieve effective lightning protection for the double-circuit distribution system while minimizing installation costs, which will be discussed in the following sections.

The waveform feature of LIOV along Line II, as shown in Fig. 12, results from a lightning stroke at Phase A between Pole 2 and Pole 3 on Line I. The waveform at Pole 2 and Pole 3, closest to the lightning stroke, exhibits a distinct negative polarity. From Pole 4 onwards, the negative polarity of the waveform becomes less pronounced, and by Pole 5, the waveform shifts from zero to a positive polarity, instead of continuing towards a negative one. The waveforms from Pole 6 to Pole 15 clearly exhibit a positive polarity. It is evident that, upon lightning impacting Line I, the main peak of the waveform near the stroke point on Line II is negative, while the main peak of the insulator waveform at poles farther from the stroke point is positive.

4.2. Combined protection of SAs and SW

A lightning stroke, occurring on the central SW between Pole 9 and Pole 10 of Line I, induces variations in the peak of the LIOV along the poles of Line II. With different grounding intervals of the SW in Line I, namely, spanning three poles and one pole, LIOV along the poles of Line II varies depending on the current magnitude, as shown in Fig. 13. The grounding resistance in these cases is 15 Ω. The solid lines represent the configuration where SAs are installed on poles spanning every other pole in Line I, whereas the dashed lines correspond to the setup where SAs are placed on poles spanning every three poles.

As shown in Fig. 13(a), the LIOV along Line II induced by the 10 kA first return stroke shows predominantly negative polarity. The highest amplitude of the LIOV appears in Phase A of Pole 9, and as the distance increases from the stroke point, the amplitude gradually decreases towards both ends of Line II. For poles closer to the stroke point, Phase A exhibits the highest amplitude, while Phase C remains the lowest. Whereas, at greater distances, the highest amplitude does not always occur in Phase A. As the distance increases, inter-phase electromagnetic coupling and reflected wave superposition are likely the primary factors influencing this variation. A first return stroke current of 80 kA causes a negative LIOV at Pole 9 and Pole 10, which are closest to the stroke point, as depicted in Fig. 13(b). On poles farther

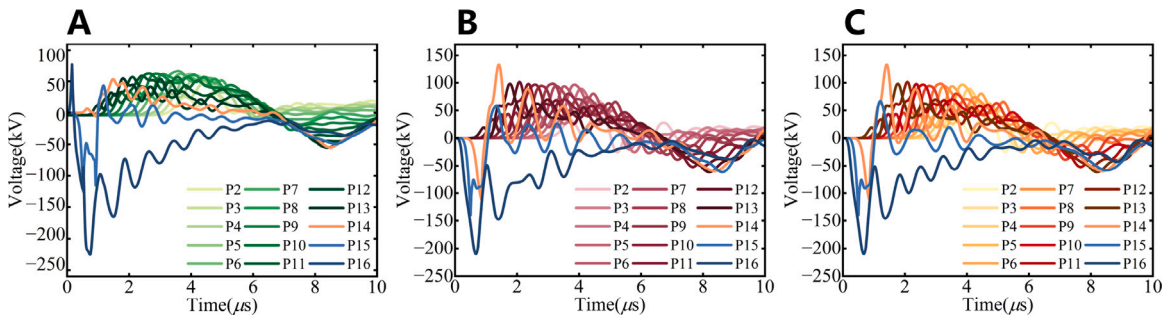

Fig. 10. Waveform features of the LIOV along the Line II with a 50 kA subsequent return stroke at Pole 16, for different SA configurations. (a) Span three poles, (b) Span two poles and (c) Span one pole.

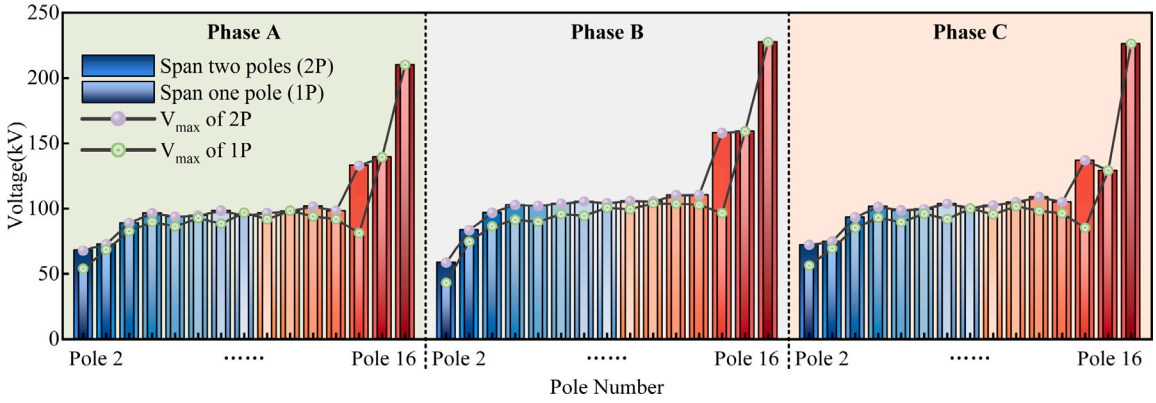

Fig. 11. Comparison of LIOV amplitudes for each phase of the poles of Line II, with configuration of spanning two poles and spanning one pole.

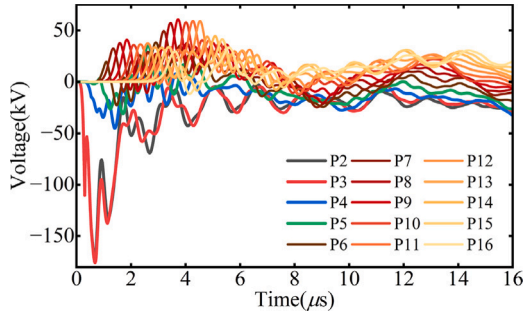

Fig. 12. Waveform features of the LIOV along the Line II with a 50 kA subsequent return stroke at the Phase A between Pole 2 and Pole 3 on Line I, with SAs installed across two-pole span.

from the stroke point, the LIOV shifts predominantly to a positive polarity.

Configuring SAs on every other pole of Line I provides better protection for Line II. When the lightning current increases to 80 kA, FO occur at Poles 6, 9, 10, 12, and 13 of Line II under the configuration where SAs are installed every three poles. In contrast, with SAs installed on every other pole, FO are limited to Pole 9 and Pole 10 of Line II.

The Flashover Rate (FOR) of the insulators along Line II under different SW configurations is shown in Fig. 14, where the grounding resistance is set to 15 Ω. According to Table 6, the cases are categorized into six types, including (a) SW grounded every three spans with SAs installed every three spans (3SW-3SA), (b) SW grounded every three spans with SAs installed every span (3SW-1SA), (c) SW grounded every span with SAs installed every three spans (1SW-3SA), (d) SW grounded every span with SAs installed every span (1SW-1SA), (e) SW grounded at every pole with SAs installed every three spans (SW-3SA), and (f) SW grounded at every pole with SAs installed every span (SW-1SA).

A FOR closer to 1 indicates a lower lightning withstand level and weaker protection performance under that configuration. As illustrated in Fig. 14(a), when the first-return stroke does not exceed 80 kA, grounding the SW at every pole significantly reduces the amplitude of LIOV along Line II, namely, reducing the grounding interval of the SW effectively decreases the flashover rate of Line II. Nevertheless, when the subsequent return stroke serves as the intrusion source, none of the configurations can effectively reduce the LIOV amplitude of Line II unless the lightning current is no greater than 50 kA.

As the SA installation density increases, the FOR gradually decreases, indicating that a higher SA installation density enhances the overall lightning withstand capability of Line II. Notably, when SAs are installed on every other pole of Line I, the grounding interval of the SW has a reduced impact on LIOV along the line. The protective effect of SAs surpasses that of the SW in improving line protection. The 30% flashover rate reduction under 80 kA strokes with one-pole SA and one-pole SW as shown in Fig. 14 arises from SW's shielding effect reducing direct coupling and SA's clamping effect limiting voltage peaks. SW grounded at one-pole intervals outperforms three-pole intervals by providing more uniform shielding as seen in lower overvoltage at Pole 9 and Pole 10 as shown in Fig. 13(b). This synergistic effect is more pronounced than individual strategies, confirming the observation from Christodoulou et al. [27], in which integrated SAs and SW systems outperform single measures though our 10 kV setup shows higher sensitivity to interval spacing than their 150 kV lines.

4.3. Grounding resistance

Both SA and SW must be grounded, making the grounding resistance at the pole a critical parameter in protection design. The influence of grounding resistance on the lightning withstand capability of distribution lines under various protection strategies is what this section delves into.

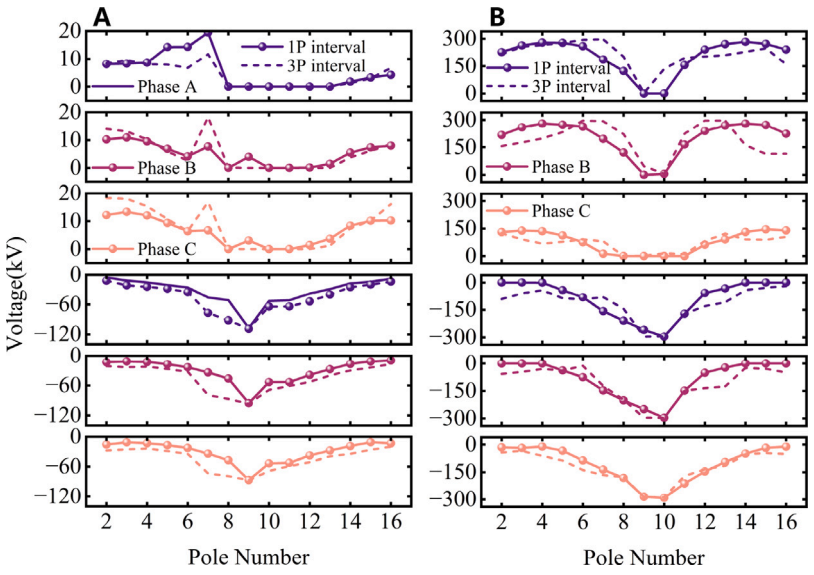

Fig. 13. LIOV phase voltage of Line II under different lightning on the central SW between Pole 9 and Pole 10 of Line I, with (a) a 10 kV first-return stroke, and (b) a 80 kV first-return stroke. (R_g = 15 Ω).

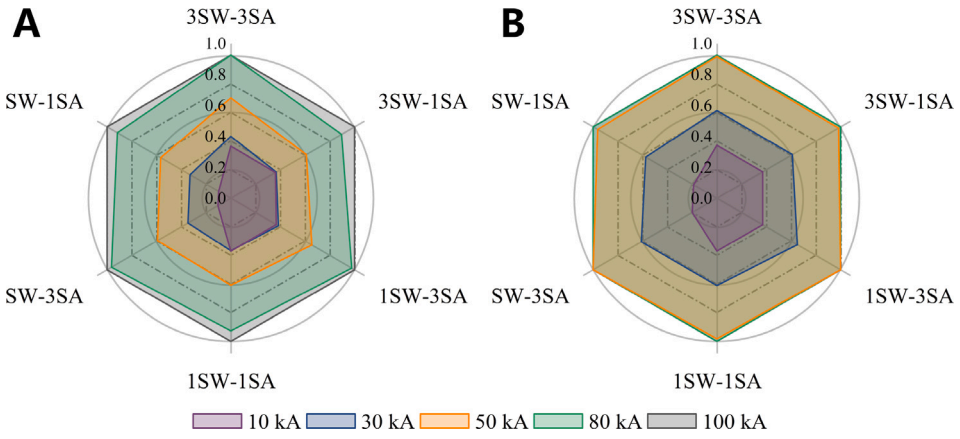

Fig. 14. Variation of FOR of Line II in different lightning current under the combined protection of different SAs configurations and SW grounding methods, with (a) first-return strokes and (b) subsequent return strokes. (R_g = 15 Ω).

Fig. 15 illustrates the impact of grounding resistance on the FOR under the first-return stroke, considering eight different protection strategies. Notably, two additional configurations are introduced, which are (g) SA installed every three spans (3SA), and (h) SA installed every span (1SA). The grounding resistance varies from 10 to 100 Ω, with 30 Ω being a reference design value adopted by the local power company [39], which is also incorporated into our analysis.

Regardless of the grounding span of the SW, the impact of grounding resistance on LIOV of Line II remains minimal when SAs are installed on every three spans of Line I, where the current peak of the SAs at both ends of Line II consistently stays below 1 kA. Interestingly, when SAs are installed on every pole of Line I, the FOR is lower with the SW grounded every three spans than with the SW grounded every pole, which is contrary to the results observed when SAs are installed every three spans. Moreover, in this configuration, as long as the SW is not grounded at every pole, its grounding span has a less significant effect on LIOV along Line II. For currents less than 80 kA, the effect of grounding resistance changes on overvoltage is less than 10%, but for lightning strokes of 80 kA, the effect is more than 20%. Therefore, in high-risk areas, if the combined protection of SAs and SW cannot be achieved, reducing the grounding resistance as much as possible can achieve better protection effects.

5. Selection of protection strategies

Based on the analysis in the previous section, SAs demonstrate superior protection for distribution lines compared to SW. Installing SAs on each pole represents the optimal lightning protection strategy. However, the cost of installing SAs on every pole is considerably high, while the frequency of damage and replacement due to lightning strokes further amplifies the economic burden. It is crucial to find a balance between protection effectiveness and cost efficiency when selecting a protection strategy. The feasible lightning protection strategies derived from the aforementioned analysis are summarized in Table 7.

To assess the performance of different lightning protection strategies, the lightning withstand level of the line is introduced as an evaluation criterion, referring to the maximum lightning current intensity that a distribution line can withstand without experiencing damage or FO during a lightning stroke. The lightning withstand levels of Line II under varying grounding resistances in the regular configuration are shown in Table 8.

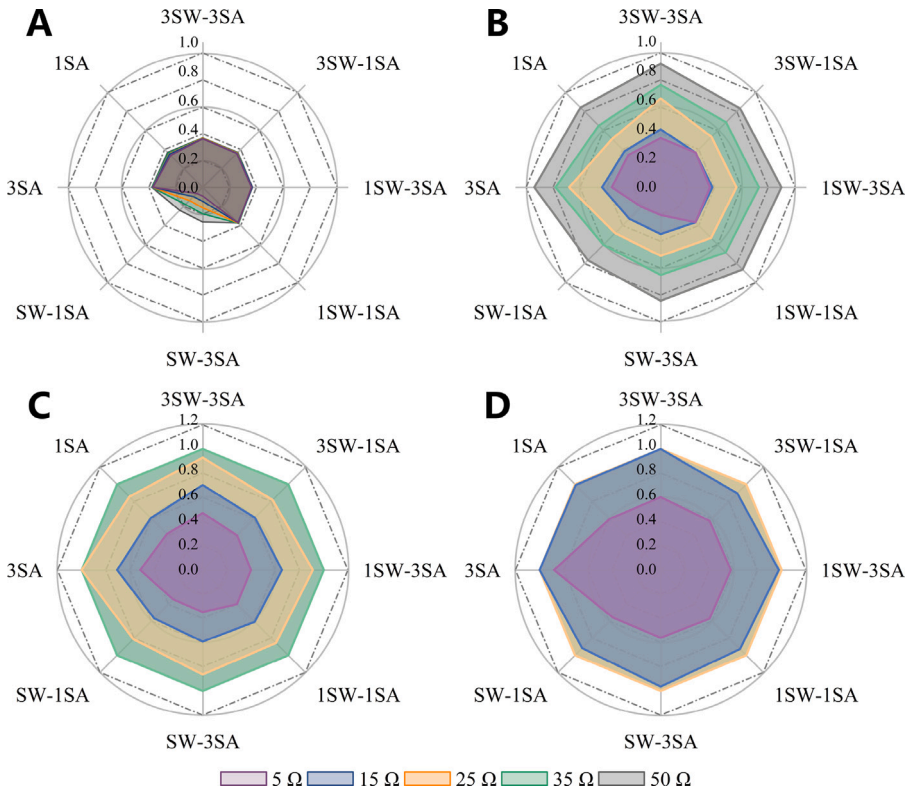

Fig. 15. Variation of FOR of Line II in different grounding resistance under the combined protection of different SAs configurations and SW grounding methods, with (a) to (d) represent 10 kV, 30 kV, 50 kV and 80 kV, respectively.

Table 7
Lightning protection strategies and specific installation measures.

Lightning protection strategy	Specific measures
Strategy 1	Install SA every span of one pole
Strategy 2	Install SA every span of one pole and SW
Strategy 3	Install SA every span of one pole and reduce grounding resistance
Strategy 4	Install SW and reduce grounding resistance
Strategy 5	Install SA every span of one pole and SW, with reducing grounding resistance

Table 8
Lightning withstand level of Line II under regular configuration of circuit I, with different lightning stroke.

Lightning stroke on lines				
Stroke point	S2		S4	
R_g	1FO (kA)	2FO (kA)	1FO (kA)	2FO (kA)
5	1.7	69.2	1.7	69.2
15	1.7	58.5	1.7	58.5
25	1.7	49.2	1.7	49.2
35	1.7	41.3	1.7	38.3
50	1.6	32.9	1.2	29.3
Lightning stroke on poles				
Stroke point	S1		S3	
R_g	1FO (kA)	2FO (kA)	1FO (kA)	2FO (kA)
5	15.9	45.7	16.0	58.5
15	14.2	38.3	12.8	41.3
25	13.2	34.5	12.4	30.5
35	12.5	30.3	10.3	29.4
50	12.0	28.3	8.5	22.9

Table 9
Lightning withstand levels of Line II under different SA configurations, without installing SW.

Configuration of SAs	Lightning stroke point			
	Stroke at Phase A between Poles 11 and 12		Stroke at P16	
	1FO (kA)	2FO (kA)	1FO (kA)	2FO (kA)
Span three poles	1.7	48.4	10.1	39.0
Span two poles	2.2	48.5	13.1	44.4
Span one pole	3.9	44.5	14.9	44.4

The lightning withstand levels at the lightning stroke points S2 and S4 are quite similar, while the impact of varying grounding resistances on the lightning withstand level leading to FO of one phase in both lines (1FO) is relatively small. Taking S2 as an example, the lightning withstand level during 1FO is less than 2 kA. When the grounding resistance is 5 Ω, the lightning withstand level during two phases in both lines (2FO) is 69.2 kA, and when the grounding resistance is 50 Ω, the lightning withstand level decreases to 32.9 kA.

In the case of a lightning stroke at the poles, there is a significant variation in the lightning withstand levels of Line II, such as S1 and S3, although all are within 16 kA. The lightning withstand level during 1FO at the pole is higher than that during a stroke on the line. However, the lightning withstand level during 2FO is lower than that during a stroke on the line. This difference diminishes as the grounding resistance increases. Note that, the analysis focuses solely on the lightning withstand levels under a grounding resistance of 25 Ω, specifically for the stroke

Table 10
Lightning withstand levels under different grounding methods for SW and SAs configurations.

Grounding method of SW	Configuration of SAs	Lightning withstand level (kA)	
		1FO	2FO
Span three poles	No SA	38.7	/
	Span three poles	40.5	41.1
	Span two poles	41.1	43.9
	Span one pole	42.7	45.5
Span one pole	No SA	39.5	/
	Span three poles	41.3	42.0
	Span two poles	41.9	45.2
	Span one pole	44.2	47.1
Every pole	No SA	40.3	/
	Span three poles	42.5	45.9
	Span two poles	43.8	48.4
	Span one pole	46.4	49.8

Table 11
Expense comparison of different lightning protection strategies.

Strategy	Cost price/US$
Strategy 1	Only installing SAs: $50/SA.
Strategy 2	Installing SAs and SW: $50/SA, and $2000/km.
Strategy 3	Installing SAs and grounding resistance: $50/SA + $300/$R_g$.
Strategy 4	Installing SW and grounding resistance: $2000/km + $300/$R_g$.
Strategy 5	Installing SAs, SW, and grounding resistance: $50/SA + $2000/km + $300/$R_g$.

at Pole 11 and Pole 12 in the central Phase A, as well as for the stroke at Pole 16 on Line I.

The lightning withstand levels under different SAs configurations are shown in Table 9. When a lightning stroke occurs on the line, increasing the density of SAs on Line I can raise the lightning withstand level during 1FO from 1.7 kA to 6.3 kA. Whereas, it does not necessarily improve the lightning withstand level during 2FO. In the case of a lightning stroke at the pole, the lightning withstand level during 1FO increases from 10.1 kA to 15.6 kA, while the lightning withstand level during 2FO rises from 36.2 kA to 44.4 kA.

The lightning withstand levels of the line under different grounding configurations of the SW and the SAs every three-pole span configuration are shown in Table 10. In this case, the lightning stroke occurs at the central SW between Pole 9 and Pole 10 on Line I. Grounding the SW at each pole increases the lightning withstand level during 1FO from 40.5 kA, with three-pole span grounding, to 42.5 kA. The lightning withstand level during 2FO rises from 41.1 kA to 45.9 kA. The addition of the SW significantly improves the lightning withstand level during 1FO, but the lightning withstand level during 2FO decreases. When only the SW is installed, the lightning withstand level during 1FO is 40.3 kA. After installing additional SAs, the lightning withstand level is further improved, with an increase of approximately 5.46% to 15.14%. Drawing from the preceding analysis, Strategy 5 demonstrates the most optimal lightning protection performance, whereas Strategy 1 exhibits the least effective protection. Additionally, under the condition of incorporating SA, reducing the grounding resistance yields a less significant protective effect when compared to the implementation of SW.

The costs of different protection strategies, according to the data provided in [40], can be quantified without considering the discount rate, as shown in Table 11. The previously mentioned strategy allows for a comprehensive evaluation of protection schemes from both the protection performance and overall cost perspectives. Note that, the cost analysis in this study is limited to the initial installation expenses of the protection strategies. Long-term factors such as the aging of SAs and SW, their maintenance frequency, replacement costs due to degradation, and performance changes caused by environmental factors are not included herein.

In summary, under the above five lightning protection strategies, the lightning withstand levels of the double-circuit distribution system remain within an acceptable range. Thus, if system cost is the primary consideration, Strategy 1 may be selected. Should system stability and safety take precedence, Strategy 5 would be the optimal choice. For a balanced consideration of both cost and stability, Strategy 2 presents a viable solution. For a comprehensive protection scheme, SW is recommended to be grounded at specified intervals to ensure basic shielding effectiveness. Regarding SA installation, regional differentiation is advised. In high-lightning-risk regions with annual lightning density greater than 20 flashes/km^2, SAs should be deployed at one-pole intervals to maximize protection. In moderate-risk regions with annual lightning density between 5 and 20 flashes/km^2, two-pole intervals for SAs balance performance and cost. In low-risk regions with annual lightning density less than 5 flashes/km^2, three-pole intervals suffice.

6. Conclusion

To address the research gaps in existing literature regarding the integrated effects of grounding, Surge Arresters (SAs), and Shielding Wire (SW) as well as differentiated protection strategies in double-circuit lines, this paper conducted an investigation into the characteristics of Lightning-induced Overvoltage (LIOV) on a 10 kV double-circuit overhead line in a distribution system under direct lightning stroke conditions. A hybrid simulation model, based on the Variable Time Step and Partial Element Equivalent Circuit (VTS-PEEC) method, is adopted to systematically analyze the influence of lightning conditions, grounding configurations, and various lightning protection strategies on the LIOV of Line II. Also, discussion about the effectiveness and economy of different lightning protection strategies is also presented.

The findings indicate that properly arranged SAs with one-pole intervals enhance one-phase flashover withstand level from 1.7 kA to 3.9 kA, and outperforming SW alone where three-pole grounded SW achieve 38.7 kA for one-phase flashover. Increasing SA density from three-pole to one-pole intervals reduces flashover rates by 30%. Combining one-pole SAs with one-pole grounded SW raises two-phase flashover withstand level to 49.8 kA while balancing economic costs. For practical applications, all SW are recommended to be grounded at specified intervals to ensure basic shielding effectiveness, with regional differentiation for SA installation. In high-lightning-risk regions, SAs should be deployed at one-pole intervals to maximize protection, while in moderate-risk regions, two-pole intervals for SAs balance performance and cost. Note that three-pole intervals suffice in low-risk regions.

Where economic conditions permit, adopting the recommended SA density combined with grounded SW achieves the optimum balance between economic efficiency and reliability. If such conditions are not met, increasing SA density alone can still enhance lightning protection. The simulation method and calculation results proposed in this paper will help investigate the lightning response of double-circuit distribution lines and provide technical support for distribution system lightning protection. However, this study has some limitations in modeling that simplify some of the models and lightning channels. Future research will focus on refining the lightning channel model and expanding the economic analysis, as well as validating these simulation results through field testing in real configurations to improve engineering applicability.

CRediT authorship contribution statement

Chakhung Yeung: Writing – original draft, Visualization, Validation, Software, Resources, Methodology, Investigation, Formal analysis, Data curation, Conceptualization. **Yuxuan Ding:** Writing – review

& editing, Supervision, Software, Methodology, Data curation. **Quan Zhou:** Writing – original draft, Visualization, Validation, Software, Methodology, Formal analysis, Data curation. **Yaping Du:** Writing – review & editing, Supervision. **Huaifei Chen:** Writing – review & editing, Software. **Lei Jia:** Supervision, Funding acquisition. **Song Zhang:** Methodology, Investigation, Funding acquisition, Formal analysis. **Yue Li:** Writing – review & editing, Validation, Data curation.

Declaration of competing interest

We declare that we have no financial and personal relationships with other people or organizations that can inappropriately influence our work, there is no professional or other personal interest of any nature or kind in any product, service and/or company that could be construed as influencing the position presented in, or the review of, the manuscript entitled.

Data availability

The data that has been used is confidential.

References

[1] Cao J, Du Y, Ding Y, Li Z, Chen M, Qi R. Performance against direct lightning on 10-kV overhead distribution lines with counterpoise wires. IEEE Trans Electromagn Compat 2023;65(4):1108–16.

[2] Cai L, Xu C, Wang J, Chu W, Zhou M, Fan Y, Cao J. Three-phase overvoltage induced on overhead distribution line 40 m from rocket-triggered lightning. IEEE Trans Power Deliv 2023;38(6):3782–91.

[3] Yeung C, Wang J, Zhou M, Zhao W, Huang W, Cao J, Cai L, Du Y. Affection of shielding methods on the characteristics for cable coupled to lightning impulse magnetic field. Electr Power Syst Res 2024;226:109802.

[4] Michishita K, Ishii M, Asakawa A, Yokoyama S, Kami K. Voltage induced on a test distribution line by negative winter lightning strokes to a tall structure. IEEE Trans Electromagn Compat 2003;45(1):135–40.

[5] Santos MN, Piantini A. Analysis of lightning-induced voltages on a matched experimental overhead line. IEEE Trans Electromagn Compat 2021;64(1):158–65.

[6] Cai L, Xu C, Cao J, Chu W, Wang J, Zhou M, Fan Y. Distribution characteristics of induced overvoltage along 10 kV distribution line caused by artificially triggered lightning at 40 m. IEEE Trans Electromagn Compat 2023;66(1):195–203.

[7] Yeung C, Wang J, Du Y, Cao J, Zhou Q, Du Z, Fan Y, Ding Y, Cai L. Clearness index cluster analysis for photovoltaic weather classification based on solar irradiation measurement data: Theory and application. Energy 360 2024;2:100010.

[8] Yeung C, Wang J, Du Y, Cao J, Zhou Q, Ding Y, Chen M, Zhao W, Jia C. Comprehensive analysis of solar irradiance and photovoltaic power generation: Case studies in Wuhan and Zhangbei, China. IEEE Trans Ind Appl 2025.

[9] Yeung C, Wang J, Du Y, Zhou M, Zhou Q, Cai L, Ding Y, Cao J, Chen M. Multi-factorial assessment of inclined surface solar radiation using photovoltaic data and solar radiation transposition models: a case study in china. Energy 360 2025;100036.

[10] Yokoyama S, Miyake K, Mitani H, Yamazaki N. Advanced observations of lightning induced voltage on power distribution lines. IEEE Trans Power Deliv 1986;1(2):129–39.

[11] Paolone M, Nucci CA, Petrache E, Rachidi F. Mitigation of lightning-induced overvoltages in medium voltage distribution lines by means of periodical grounding of shielding wires and of surge arresters: Modeling and experimental validation. IEEE Trans Power Deliv 2004;19(1):423–31.

[12] Cao J, Ding Y, Du Y, Chen M, Qi R. Design consideration of the shielding wire in 10 kV overhead distribution lines against lightning-induced overvoltage. IEEE Trans Power Deliv 2020;36(5):3005–13.

[13] Yeung C, Wang J, Zhou M, Cao J, Ding Y, Cai L, Fan Y, Zhou Q, Wang J, Zhao W. Transient induced response on cables by lightning electromagnetic pulse with different experimental conditions. Electr Power Syst Res 2025;238:111031.

[14] Cao J, Xu C, Cai L, Wang J, Zhou M, Chu W, Zhao W, Yeung C. Observed induced overvoltage on the test overhead distribution initiated from natural lightning activities. In: 2024 IEEE/IAS 60th industrial and commercial power systems technical conference. I&CPS, IEEE; 2024, p. 1–6.

[15] Yeung C, Wang J, Du Y, Zhou M, Cai L, Cao J, Zhou Q, Ding Y, Zhao W, Chen M. Assessment of electromagnetic shielding effectiveness in multi-layer and single-layer shielded cables against the lightning electromagnetic pulse considering different shielding strategies. Electr Power Syst Res 2025;243:111514.

[16] Baba Y, Nagaoka N, Ametani A. Modeling of thin wires in a lossy medium for FDTD simulations. IEEE Trans Electromagn Compat 2005;47(1):54–60.

[17] He J, Hu J, Gu S, Zhang B, Zeng R. Analysis and improvement of potential distribution of 1000-kV ultra-high-voltage metal–oxide arrester. IEEE Trans Power Deliv 2009;24(3):1225–33.

[18] Shafieipour M, Nazari M, Dawalibi FP, Fortin S, Tatematsu A, De Silva J, Gómez P. Full-wave 3-D transient analysis with method of moments and numerical Laplace transform including resistive non-linear elements. IEEE Trans Power Deliv 2022;38(1):299–308.

[19] Yeung C, Lyu J, Du Y, Zhou Q, Wang M, Jia L, Chen X, Qi R, Xiao X, Li Y. Methodology for fast impedance calculation for twisted power cables at high-frequency via a multi-level PEEC method. IEEE Trans Ind Appl 2025.

[20] Diendorfer G. Induced voltage on an overhead line due to nearby lightning. IEEE Trans Electromagn Compat 1990;32(4):292–9.

[21] Nucci CA, Rachidi F, Ianoz MV, Mazzetti C. Lightning-induced voltages on overhead lines. IEEE Trans Electromagn Compat 1993;35(1):75–86.

[22] Nucci CA, Guerrieri S, De Barros MC, Rachidi F. Influence of corona on the voltages induced by nearby lightning on overhead distribution lines. IEEE Trans Power Deliv 2000;15(4):1265–73.

[23] Ishii M, Michishita K, Hongo Y, Oguma S. Lightning-induced voltage on an overhead wire dependent on ground conductivity. IEEE Trans Power Deliv 1994;9(1):109–18.

[24] Rachidi F, Rubinstein M, Guerrieri S, Nucci CA. Voltages induced on overhead lines by dart leaders and subsequent return strokes in natural and rocket-triggered lightning. IEEE Trans Electromagn Compat 1997;39(2):160–6.

[25] Paulino JOS, Barbosa CF, da Silva Lopes IJ, de Miranda GC. Time-domain analysis of rocket-triggered lightning-induced surges on an overhead line. IEEE Trans Electromagn Compat 2009;51(3):725–32.

[26] Cao J, Du Y, Ding Y, Li B, Qi R, Zhang Y, Li Z. Lightning surge analysis of transmission line towers with a hybrid FDTD-PEEC method. IEEE Trans Power Deliv 2021;37(2):1275–84.

[27] Christodoulou C, Ekonomou L, Fotis G, Harkiolakis N, Stathopulos I. Optimization of Hellenic overhead high-voltage transmission lines lightning protection. Energy 2009;34(4):502–9.

[28] Ekonomou L, Fotis G, Maris T. Cost related optimum design method for overhead high voltage transmission lines. Eur Trans Electr Power 2008;18(5):437–47.

[29] Cao J, Du Y, Ding Y, Qi R, Chen M, Li Z, Zhao X, Andreotti A. Lightning protection with a differentiated configuration of arresters in a distribution network. IEEE Trans Power Deliv 2022;38(1):409–19.

[30] Zhao Y, Wang J, Cai L, Li Q, Zhou M, Su R, Xu Z, Fan Y. Induced voltage at two poles of 10kV parallel distribution line caused by direct lightning strike on the phase wire of adjacent line. Electr Power Syst Res 2022;211:108215.

[31] Yeung C, Ding Y, Zhou Q, Du Y, Zhang S, Qi R, Jia L. An accelerated multi-time-scale solution of power systems under multiple lightning strokes events. IEEE Trans Power Deliv 2025;40(4):1889–98.

[32] Cao J, Du Y, Ding Y, Qi R, Li B, Chen M, Li Z. Practical schemes on lightning energy suppression in arresters for transformers on 10 kV overhead distribution lines. IEEE Trans Power Deliv 2022;37(5):4272–81.

[33] Paul CR. Analysis of multiconductor transmission lines. John Wiley & Sons; 2007.

[34] Rachidi F, Loyka S, Nucci C, Ianoz M. A new expression for the ground transient resistance matrix elements of multiconductor overhead transmission lines. Electr Power Syst Res 2003;65(1):41–6.

[35] Piantini A, Janiszewski JM, Borghetti A, Nucci CA, Paolone M. A scale model for the study of the LEMP response of complex power distribution networks. IEEE Trans Power Deliv 2006;22(1):710–20.

[36] Martinez J, Durbak D. Parameter determination for modeling systems transients-Part V: Surge arresters. IEEE Trans Power Deliv 2005;20(3):2073–8.

[37] IEEE guide for improving the lightning performance of electric power overhead distribution lines. In: IEEE Std 1410-2010 (revision IEEE std 1410-2004). IEEE; 2011, p. 1–73.

[38] Heidler F, Cvetic J, Stanic B. Calculation of lightning current parameters. IEEE Trans Power Deliv 1999;14(2):399–404.

[39] Code for design of 66 kV or under overhead electrical power transmission line. 2010, China Standard GB 50061-2010.

[40] Gao Y, Han Y, Xiao F, Chen C, Zhang J, Zhang J, Zhang Y, Li L. Study on lightning protection scheme of multi-terminal MMC-MVDC distribution system. High Volt 2020;5(5):605–13.